

# Structured Volume Decomposition via Generalized Sweeping

## Supplemental material - extensions and additional results

Xifeng Gao, Tobias Martin, Sai Deng, Elaine Cohen, Zhigang Deng, and Guoning Chen

### 1 IMPROVED BIFURCATION HANDLING

As illustrated in the paper that the basic bifurcation handling introduces two valence-6 extraordinary points on the surface, which may result in elements with large distortion. To improve the element quality at bifurcations, we extend the bifurcation handling as follows.

**1.** Instead of computing the line segment  $R_0R_1$  crossing the saddle point, we first find a surface patch  $R_0R_1R_2R_3$  that covers the bifurcation (i.e., the purple patch in Figure 1(a)). To achieve that, the user specifies the four points,  $R_0$ ,  $R_1$ ,  $R_2$ ,  $R_3$ , at the boundary of level set  $\mathcal{L}_i$ . Then, the shortest surface curves connecting  $R_0$ ,  $R_3$  and  $R_1$ ,  $R_2$  are computed, respectively. This step can also be automatically achieved by the following steps: 1) computing the line segment  $R'_0R'_1$  crossing the saddle point; 2) using  $R'_0$  and  $R'_1$  as the center of edges  $P_1P_4$  and  $P_2P_3$  of  $Q_i$ , find  $R_0R_1$  and  $R_2R_3$  to make sure  $R_0$  and  $R_1$  are at the two sides of  $R'_0$ , and,  $R_2$  and  $R_3$  are at the two sides of  $R'_1$ . Distances of  $R_0$  and  $R_1$  from  $R'_0$  are the same, which are  $1/3$  of the segment length  $P_1R'_0$  and  $R'_0P_4$ , respectively. These are the same for  $R_2$  and  $R_3$  as well.

**2.** Next, similar to the original pipeline, we project  $R_0, R_1, R_2, R_3$  along the inverse gradient direction of the harmonic field to obtain  $P_0, P_1, P_2, P_3$ . Together, these eight points form a hexahedral component (Figure 1(b)). When connecting the patches of  $\mathcal{Q}^{i+1,0}$  and  $\mathcal{Q}^{i+1,1}$  with those of  $\mathcal{Q}^i$ , rather than mapping the two unmatched patches to a single section, i.e.,  $R_0P_0P_1R_1$  in Figure 7(c), we now map them to two sections, i.e.,  $R_0P_0P_3R_3$  and  $R_1P_1P_2R_2$ , respectively, as shown in

Figure 1(c). Through the above process, the two valence-6 extraordinary points are split into four valence-5 extraordinary points, corresponding to  $R_0, R_1, R_2, R_3$ , respectively.

**3.** By propagating this splitting operation down (splitting bifurcation) or up (merging bifurcation) throughout the whole mesh, a new hex patch in the base-complex can be generated.

Note that this extended bifurcation handling is an optional process that is suitable to the bifurcations whose neighborhoods are relatively flat, such as the back of the kitten model. In our results, this process has only been applied to the kitten, fertility, blade, and rocker arm models.

### 2 SPLINE FITTING

To fit the splines, for each hexahedral component (i.e. a cuboid) in the hex mesh representation, we compute a regular grid of control points, i.e., sub-dividing the cuboid along each dimension evenly. Due to the higher degree used in the B-spline basis, regular sampling, as used for a trilinear basis causes distortion. A bijective mapping can be computed which maps from the unit cube,  $\mathbf{C} : [0, 1] \times [0, 1] \times [0, 1]$ , to the corresponding hexahedral component  $\mathcal{C}$ , i.e.  $f : \mathbf{C} \rightarrow \mathcal{C}$ . We regularly place samples  $\mathbf{C}$  along each dimension, which gives rise to a set of 3D grid points  $\mathbf{P}_i$ . These points are then mapped back to the space of  $\mathcal{C}$  via the inverse function  $f^{-1}$ . This returns the samples in  $\mathcal{C}$ , denoted by  $\mathcal{P}_i$ . They are the control points for the spline fitting. This process is the Schoenberg approximation in the context of data fitting.

After computing the node locations, trilinear B-spline patches can be fitted to each of the cuboids individually using standard fitting methods as used in [1]. The smoothness of the fitted spline is  $C^2$  in the interior of each patch but  $C^0$  across the boundaries. It should

• Xifeng Gao, Zhigang Deng, and Guoning Chen are with the Department of Computer Science, University of Houston.  
 • Tobias Martin is with ETH Zürich.  
 • Sai Deng and Elaine Cohen are with the School of Computing, University of Utah.

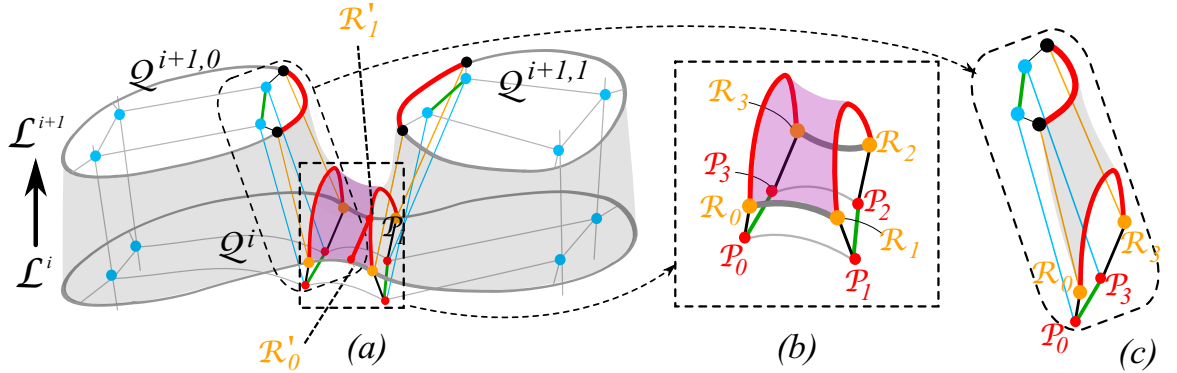


Fig. 1. Illustration of the extended bifurcation handling: (a) the configuration at a splitting bifurcation in the extended process, (b) a new hexahedral component formed by the new saddle patch, and (c) the mapping of the unmatched patch in  $Q^{i+1,0}$  to the section  $R_0 P_0 P_3 R_3$ .

be clarified that our focus is not to achieve higher-order smoothness across the boundaries of cuboids. However, the predictable and simple structure of our output potentially allows us to increase the continuity by reducing the number of boundaries between patches. Even so, the smoothness around the neighborhood of an extraordinary point is not guaranteed, and can be at most  $C^0$ . Methods like SRF and Polycube approaches introduce larger number of hexahedral components, reducing the continuity over the space as only  $C^0$  smoothness can be guaranteed across the cuboid boundaries.

### 3 ADDITIONAL RESULTS

Figures 2 and 3 provide a gallery of the additional results generated with our method.

### REFERENCES

- [1] Bo Li, Xin Li, Kexiang Wang, and Hong Qin. Surface mesh to volumetric spline conversion with generalized poly-cubes. *IEEE Trans. Vis. Comput. Graphics*, 19(9):1539–1551, 2013.

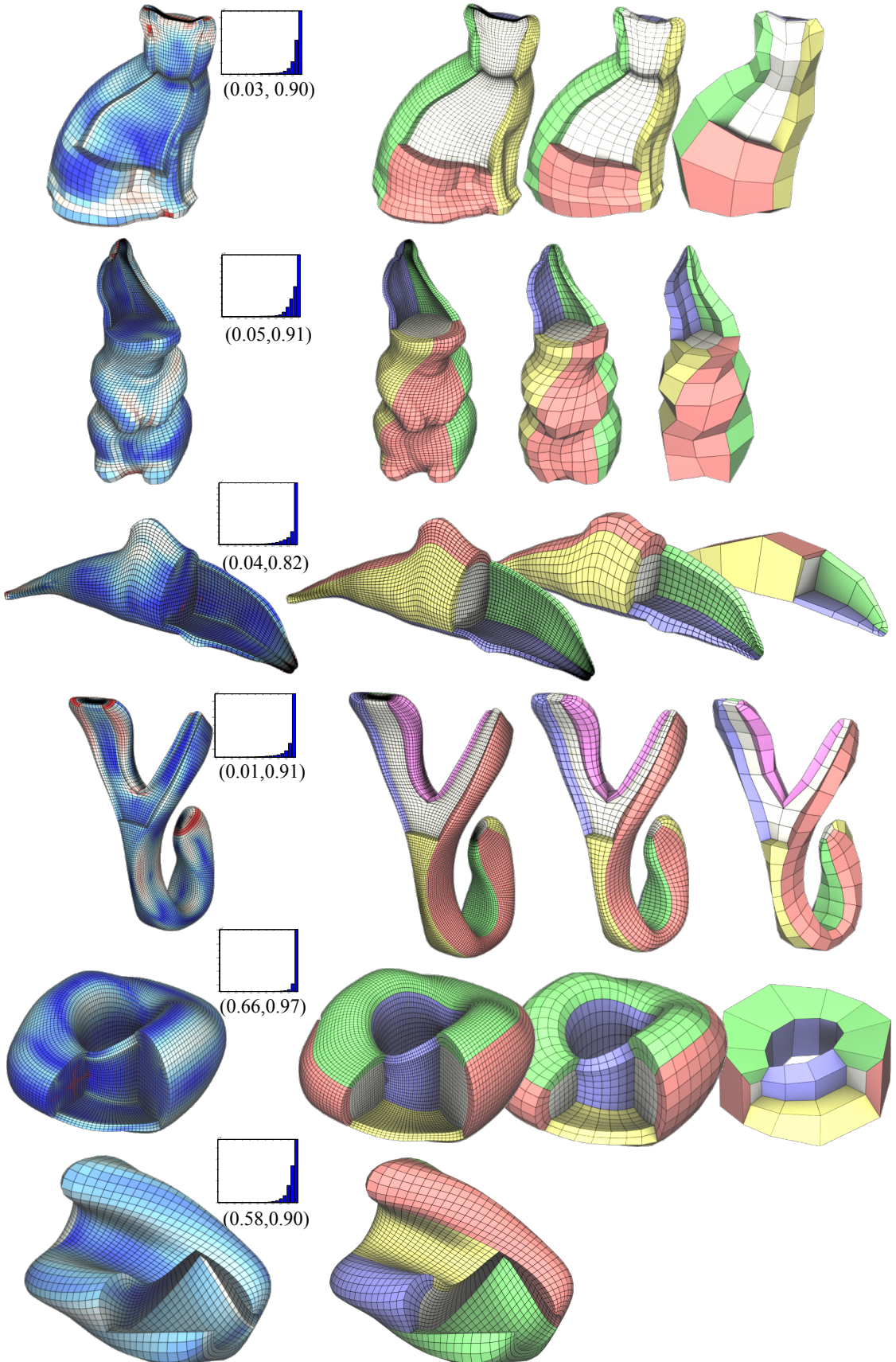


Fig. 2. Additional results for the cat, rabbit, dolphin, sculpture, deformed torus, and U-shape models with our method. The left most column shows the Jacobian visualizations and the histograms of the Jacobian distribution of the finest version of the corresponding hex-meshes. The right columns show the meshes with different resolutions. Hex-elements that belong to the same hexahedral component (see the definition in the paper) are displayed with the same color. The numbers below the histograms show the minimum and average Jacobian values.

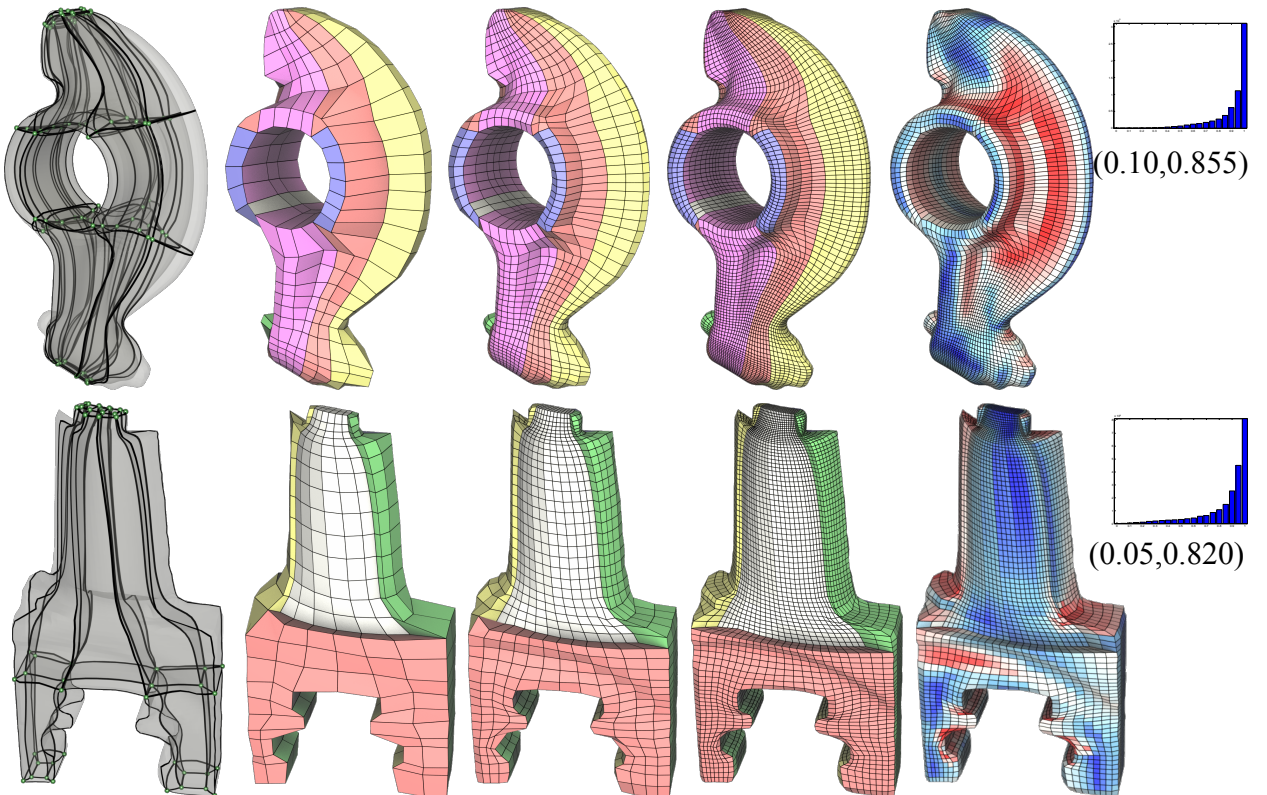


Fig. 3. Additional results for the rocker arm and a blade. Hex-elements that belong to the same hexahedral component (see the definition in the paper) are displayed with the same color. The numbers below the histograms show the minimum and average Jacobian values.